Available online at www.sciencedirect.com
ScienceDirect
Bioorganic Chemistry 35 (2007) 205–220
BIOORGANIC CHEMISTRY
www.elsevier.com/locate/bioorg

Interest of RGD-containing linear or cyclic peptide targeted tetraphenylchlorin as novel photosensitizers for selective photodynamic activity

Céline Frochot [a], Benoît Di Stasio [a,b], Régis Vanderesse [c], Marie-Josée Belgy [a], Marc Dodeller [d], François Guillemin [b], Marie-Laure Viriot [a], Muriel Barberi-Heyob [b,*]

[a] *DCPR, UMR 7630 CNRS-INPL, Groupe ENSIC, Nancy Université, 1 rue Grandville, 54000 Nancy, France*
[b] *Centre Alexis Vautrin, CRAN, UMR 7039 CNRS-UHP-INPL, Nancy Université, Av. de Bourgogne, Brabois, 54511 Vandœuvre-les-Nancy, France*
[c] *LCPM, UMR 7568 CNRS-INPL, Groupe ENSIC, Nancy Université, 1 rue Grandville, 54000 Nancy, France*
[d] *LSMCL, Université Paul Verlaine-Metz, 1 Boulevard Arago, 57078 Metz Technopole 2000 cedex 03, France*

Received 14 September 2006
Available online 9 December 2006

Abstract

Destruction of the neovasculature is essential for tumor eradication by photodynamic therapy. Since the over-expression of integrins is correlated with tumor angiogenesis, we conjugated a photosensitizer (5-(4-carboxyphenyl)-10,15,20-triphenylchlorin or porphyrin) to the $\alpha_v\beta_3$ integrin specific peptide RGD (H-Arg-Gly-Asp-OH) motif as a common sequence. We reported an efficient solid-phase synthesis of a new family of peptidic photosensitizers with linear or cyclic[RGDfK] RGD motif and compared conjugates *in vitro* selectivity and photodynamic activity. The conjugates were characterized by ^{1}H NMR, MALDI, UV–visible spectroscopy and singlet oxygen formation was performed. Chlorins containing linear and constrained RGD motif were incorporated up to 98- and 80-fold more, respectively, than the unconjugated photosensitizer over a 24-h exposure in human umbilical vein endothelial cells (HUVEC) over-expressing $\alpha_v\beta_3$ integrin. Peptidic moiety also led to a non-specific increased cellular uptake by murine mammary carcinoma cells (EMT-6), lacking RGD binding

* Corresponding author. Fax: +33 3 83 44 60 71.
E-mail address: m.barberi@nancy.fnclcc.fr (M. Barberi-Heyob).

0045-2068/$ - see front matter
doi:10.1016/j.bioorg.2006.11.005

receptors. Survival measurements demonstrated that HUVEC were greatly sensitive to conjugates-mediated photodynamic therapy.

Keywords: Chlorin; Porphyrin; RGD; Solid-phase synthesis; Singlet oxygen quantum yield; HUVEC; EMT-6; $\alpha_v\beta_3$ integrin

1. Introduction

Photodynamic therapy (PDT) is a promising treatment for a variety of oncological, cardiovascular, dermatological, and ophthalmic diseases [1]. PDT is based on the use of photosensitizers, which are preferentially taken up and/or retained by diseased tissues. It involves a photosensitizer, light, and molecular oxygen, whose combined action results in the formation of singlet oxygen, which is thought to be the main mediator of cellular death induced by PDT [2]. Normal cells, however, are also able to accumulate photosensitizers and to be damaged by them, so that prolonged skin photosensitization, light-sensitivity of the eyes and other side effects have proved to be severe limitations of PDT [3]. As a result, more selective photosensitizers, named third generation photosensitizers are desired. Until now, most of the efforts in the development of tumor targeting photosensitizers have focused on the targeting of markers over-expressed by tumor cells themselves [4]. However, PDT effects are mediated not only through direct killing of tumor cells but also through indirect effects, involving both initiation of an immune response against tumor cells and destruction of the neovasculature [5]. The latter effect may indirectly lead to tumor destruction, following lack of nutrients and oxygen. This vascular effect is thought to play a major part in the eradication of some vascularized tumors by PDT [6]. The ideal drug delivery system should enable the selective accumulation of the photosensitizer within tumoral tissue and neovasculature. The carrier must also be able to incorporate the photosensitizer without loss or alteration of its activity. In view of repetitive dosing schedules, the system must also be biodegradable and have little or no immunogenicity [7]. To this end, we have devised a synthetic route to porphyrin derivatives designed for targeting tumors and more specifically neovascularization that nourish cancer cells. Endothelial cells are crucial in angiogenesis, the process of new blood vessel formation associated with tumor growth and metastasis [8]. $\alpha_v\beta_3$ integrin, a heterodimeric transmembrane glycoprotein receptor, is over-expressed in actively proliferating endothelial cells, in and around tumor tissues [9]. Integrins are involved in cell–cell and cell–matrix interactions and in inside-out and outside-in signal transduction [10]. The $\alpha_v\beta_3$ integrin, known as the vitronectin receptor, is selectively over-expressed on the surface of endothelial cells of growing blood vessels and has been identified as a target in pathologies in which angiogenesis is stimulated [11]. In malignant tumors, $\alpha_v\beta_3$ is over-expressed in neocapillaries and in certain cases also on tumor cells. This led many groups to design ligands that could be used for drug delivery and molecular cancer imaging [12]. Among the 25 $\alpha\beta$ heterodimers, half of them bind to the common RGD motif, but RGD containing substrates have been reported to be selective for a given

integrin. The specificity of the $\alpha_v\beta_3$-RGD recognition is attributed to the sequences flanking the RGD triad, the auxiliary binding motifs in the ligand, and to a large extent, the conformational presentation of the triad [13,14]. Extensive ligand-based drug studies and rational screening of cyclic peptide libraries with constrained backbone conformations led to the discovery of the highly active and selective first-generation peptide cyclo[RGD] [13,14]. The synthetic peptide showed a higher affinity for $\alpha_v\beta_3$ than for $\alpha_v\beta_5$ or $\alpha IIb\beta_3$. Its *N*-alkylated successor cyclo[RGDf(NMe)V] has entered clinical phase II studies as an angiogenesis inhibitor [15]. In this context, this integrin may therefore represent a promising target for the delivery of drugs such as photosensitizers. We selected the well known cyclo[RGDfK] ligand, a gold-standard molecule for imaging and therapy of tumors, and used the lysine side chain to couple 5-(4-carboxyphenyl)-10,15,20-triphenylchlorin. Porphyrins or chlorins can be easily modified through a carboxyl group, which makes the compound suitable for conjugation as we recently described [16–18]. This paper reported the efficient solid-phase synthesis of a new family of chlorin (**1**) and porphyrin (**1b**) with linear RGD triad or cyclic[RGDfK] RGD motif (**2**). Conjugates selectivity and photodynamic activity were compared between $\alpha_v\beta_3$-positive HUVEC and $\alpha_v\beta_3$-negative EMT-6 cells.

2. Materials and methods

2.1. Reagents and materials

5-(4-Carboxyphenyl)-10,15,20-triphenylchlorin (TPC) and tetraphenylporphyrin (TPP) were purchased from Frontier Scientific (Logan, Utah). The Fmoc-Asp(OtBu)-Wang and H-Gly-2-chlorotrityl resins and 9-fluorenyl-methoxy-carbonyl (Fmoc)-amino acids were from Senn Chemicals International (Dielsdorf, Switzerland). Thin-layer chromatography (TLC) was carried out on Merck silica gel 60 F254 plates (Merck Chimie S.A.S., Fontenay Sous Bois, France) and developed with the appropriate solvents. The TLC spots were visualized either by UV light or by heating plates sprayed with a solution of phosphomolybdic acid (5% ethanolic solution). Chromatography column was carried out on Merck silica gel (230–400 mesh).

Assembly of the peptide chains was carried out on a multichannel peptide synthesizer, according to a classical Fmoc/*t*Bu solid-phase methodology using the *in situ* neutralization protocol [19]. For the attachment of each amino acid, double couplings (20 and 40 min, respectively) were performed using a threefold excess of *N*-Fmoc-amino acid and activation reagents 2-(1*H*-benzotriazol-1-yl)-1,1,3,3-tetramethyl-uronium tetrafluoroborate (TBTU) (3 eq.), 1-hydroxybenzotriazole (HOBt) (3 eq.) and *N*,*N*-diisopropylethylamine (DIEA) (9 eq.) in dimethylformamide (DMF). Monitoring of the reaction was performed by the 2,4,6-trinitrobenzenesulfonic acid test. For the attachment of the photosensitizer, only one coupling step using 2-fold excess was applied. During the photosensitizer coupling stage and all the next steps, light exposure was minimized by sealing the reaction vessel in foil to limit the occurrence of unwanted side reactions. Before cleavage, the peptide-resin was washed extensively with dichloromethane and dried *in vacuo*.

^{1}H NMR spectra were recorded on BRUKER AVANCE spectrometer at 300 MHz. Mass spectra analyses (MALDI-TOF) were carried out on Analyses were

performed on a Bruker Reflex IV time-of-flight mass spectrometer (Bruker-Daltonic, Bremen, Germany) equipped with the SCOUT 384 probe ion source, as described previously [17]. The system uses a pulsed nitrogen laser (337 nm, model VSL-337ND, Laser Science Inc., Boston, MA) with energy of 400 μJ/pulse. The analysis was performed in the positive mode with an acceleration voltage of 20 kV and a reflector voltage of 23 kV. The detector signals were amplified and transferred to the XACQ program on a SUN work station (Sun Microsystems Inc. Palo Alto, CA). Spectra were processed with the XMass 5.1 program (Bruker Daltonics). External calibration of MALDI mass spectra was carried out using sodic and potassic distribution with a mixture of PEG 600 and PEG 1000.

2.2. Synthesis of 5-(4-carboxyphenyl)-10,15,20-triphenylchlorin-RGD (**1**) and 5-(4-carboxyphenyl)-10,15,20-triphenylporphyrin-RGD (**1b**)

The synthesis was performed using the preloaded Fmoc-Asp(OtBu)-Wang (capacity, 0.79 mmol/g) on a 0.15 g scale. The side chains of arginine and aspartic acid were, respectively, protected by Pbf (2,2,5,7,8-pentamethylchroma-6-sulfonyl) group, and *tertio*-butyl (*t*-Bu). The successive coupling of Fmoc-Gly-OH (106 mg) and Fmoc-Arg(Pbf)-OH (230 mg) in the presence of TBTU (114 mg), BtOH (54 mg), and 0.18 mL of DIEA in 5 mL of DMF were achieved. After the final removal of the Fmoc group, the peptide-resin was washed with CH_2Cl_2 (6× 5 mL) and then dried *in vacuo* overnight. A standard cleavage with a mixture of 0.75 g of crystalline phenol, 0.25 mL of 1,2-ethanedithiol, 0.5 mL of thioanisole, 0.5 mL of deionized H_2O, and 10 mL of trifluoroacetic acid (TFA) for 1.5 h afforded the crude peptide, which was lyophilized. The compounds were purified by RP-HPLC on a C_{18} semi-preparative column (250 × 10 mm I.D., Apollo, Alltech, Lokeren, Belgium) using a 0.1% (v/v) TFA-water/acetonitrile gradient, monitored by both absorbance at 415 nm on a SPD-10A UV–visible detector (Shimadzu, France) and fluorescence on a RF 10AXL fluorescence detector (Shimadzu). After removal of the solvents, the purified compounds were lyophilized and analyzed by ^{1}H NMR and mass spectroscopy.

2.2.1. 5-(4-Carboxyphenyl)-10,15,20-triphenylchlorin-RGD (**1**)

^{1}H NMR (DMSO) δ: −1.58, −1.52 (s, 2H, NH-pyrrole), 1.50 (m, 2H, γArg), 2.30 (m, 2H, βArg), 2.18, 2.22 (m, 2H, βAsp), 3.12 (m, 2H, δArg), 4.00 (s, 1H, αGly), 4.10 (s, 1H, αAsp), 4.14 (s, 4H, CH_2-chlorin), 4.32 (s, 1H, αArg), 7.23 (s, 1H, NHε-Arg), 7.98 (s, 1H, NH-Arg), 8.20 (s, 1H, NH-Gly), 7.23–8.57 (m, 1H, ArH, pyrrole) MS (MALDI-TOFMS) *m*/*z*: calculated 989.41; found: 989.34.

2.2.2. 5-(4-Carboxyphenyl)-10,15,20-triphenylporphyrin-RGD (**1b**)

^{1}H NMR (DMSO) δ: −2.91 (s, 2H, NH-pyrrole), 1.58 (m, 2H, γArg), 2.30 (m, 2H, βArg), 2.22, 2.24 (m, 2H, βAsp), 3.12 (m, 2H, δArg), 4.02 (s, 2H, αGly), 4.12 (s, 1H, αAsp), 4.28 (s, 1H, αArg), 7.22 (s, 1H, NHε-Arg), 8.05 (s, 1H, NH-Arg), 8.25 (s, 1H, NH-Gly), 7.23–8.83 (m, 1H, ArH, pyrrole) MS (MALDI-TOFMS) *m*/*z*: calculated 987.39; found: 988.78.

2.3. Synthesis of 5-(4-carboxyphenyl)-10,15,20-triphenylchlorin-cyclo[RGDfK] (**2**)

2.3.1. Synthesis of 5,10,15,tri(p-tolyl)-20-(p-carboxyphenyl)chlorin succinidyl ester

In the dark under a nitrogen atmosphere, *N*-hydroxysuccinimide (26.1 mg, 0.23 mmol) and dicyclohexylcarbodiimide (DCC)[1] (46.8 mg, 0.23 mmol) were added to a solution of 5,10,15-tri(*p*-tolyl)-20-(*p*-carboxyphenyl)chlorin (150 mg, 0.23 mmol) in CH_2Cl_2 (6 mL). The mixture was stirred 4 h at room temperature. The solvent was evaporated and the crude material was purified by column chromatography using EtOH/CH_2Cl_2: 4/96 (v/v) as the eluent. The fractions were tested by TLC and the pure compound was isolated as a purple solid (112 mg, 65%).

^{1}H NMR (DMSO): δ −1.50, −1.65 (s, 2H, NH-pyrrole), 2.99 (s, 4H, CH_2), 4.17 (s, 4H, CH_2-chlorin), 7.26–8.85 (m, 25H, ArH, pyrrole).

2.3.2. Synthesis of 2-(9H-fluoren-9-ylmethoxycarbonylamino)-6-[5,10,15,tri(p-tolyl)-20-(p- carboxyamino)-chlorin]-hexanoic acid

In the dark under a nitrogen atmosphere, to a solution of 81 mg of Fmoc-Lys-OH, HCl (0.20 mmol) in a minimum of DMF were added *N*-hydroxysuccinimide activated chlorin (152 mg, 0.20 mmol) and triethylamine (0.20 mmol, 28.3 μL) in 10 mL CH_2Cl_2. After been stirred at ambient temperature for 24 h, the solvent was evaporated and the crude material was purified by column chromatography using EtOH/CH_2Cl_2: 5/95 (v/v) as the eluent. The fractions were tested by TLC and the pure compound was isolated as a purple solid (152 mg, 75%).

^{1}H NMR (DMSO): δ −1.58, −1.52 (s, 2H, NH-pyrrole), 1.57 (m, 2H, $CH_2\gamma$), 1.75 (m, 2H, $CH_2\delta$), 1.85, 2.00 (m, 2H, $CH_2\beta$), 3,57 (m, 1H, CHε), 4.11 (s, 4H, CH_2-chlorin), 4.14 (m, 1H, CH-Fmoc), 4.40 (m, 1H, Chα), 4.36 (s, 2H, CH_2-Fmoc), 5.76 (m, 1H, NH), 6.70 (m, 1H, NHε), 7.18–8.82 (m, 33H, ArH, pyrrole, Fmoc).

2.3.3. Synthesis of **2**

The synthesis was performed using the preloaded H-Gly-2-chlorotrityl PS resin (capacity, 0.85 mmol/g) on a 0.115 g scale. The side chains of arginine and aspartic acid were, respectively, protected by Pbf and *t*-Bu groups. The successive coupling of Fmoc-Arg(Pbf)-OH (190 mg), Fmoc-Lys(CO-Chl1)-OH (152 mg), Fmoc-(*D*)Phe-OH (114 mg) and Fmoc-Asp(OtBu)-OH (121 mg) in the presence of TBTU (94 mg), BtOH (45 mg), and 0.15 mL of DIEA were achieved. After the final removal of the Fmoc group, the peptide-resin was washed with CH_2Cl_2 (6× 5 mL) and then dried *in vacuo* overnight. The linear Chl1-CO-

[1] *Abbreviations used:* DCC, dicyclohexylcarbodiimide; DIPCDI, diisopropylcarbodiimide; DIEA, *N*,*N*-diisopropylethylamine; DMAP, 4-dimethylaminopyridine; DMF, dimethylformamide; DMSO, dimethylsulfoxide; DPPA, diphenylphosphoryl azide; EMT-6, murine mammary carcinoma; FBS, fetal bovine serum; HOBt, 1-hydroxybenzotriazole; HPLC, high-performance liquid chromatography; HOSu, *H*-hydroxysuccinimide; HUVEC, human umbilical vein endothelial cells; MALDI-TOF, matrix-assisted laser desorption ionisation time-of-flight; LD_{50}, light doses yielding 50% growth inhibition; MTT, 3-(4,5-dimethylthiazol-2-yl)-2,5-diphenyl tetrazolium bromide; $NaHCO_3$, sodium hydrogenocarbonate; NMM, *N*-methylmorpholine; Pbf, 2,2,5,7,8-pentamethylchroma-6-sulfonyl; PBS, phosphate-buffered saline, PDT, photodynamic therapy; PyBOP, benzotriazole-1-yl-oxy-tris-pyrrolidino-phosphonium hexafluorophosphate; TBTU, 2-(1*H*-benzotriazol-1-yl)-1,1,3,3-tetramethyl-uronium tetrafluoroborate; *t*-Bu, *tertio*-butyl; T3P, 1-propane-phosphonic acid cyclic anhydride; TFA, trifluoroacetic acid; TFE, 2,2,2 trifluoroethane; TLC, thin-layer chromatography; TPC, 5-(4-carboxyphenyl)-10,15,20-triphenylchlorin; TPP, tetraphenylporphyrin.

RGDfK peptide was cleaved from the resin without affecting other protecting groups with 10 mL of a mixture of acetic acid, 2,2,2 trifluoroethane (TFE) and CH_2Cl_2 (1/1/3) for 1 h at room temperature. The resin was washed with three times with acetic acid and then lyophilized. The head-to-tail cyclization was performed by slowly adding a solution of the linear peptide acetate salt in 20 mL of CH_2Cl_2 to a solution of 50% 1-propane-phosphonic acid cyclic anhydride (T3P) in EtOAc (3 mL), triethylamine (3 mL), and DMAP (10 mg) in 400 mL of CH_2Cl_2. After stirring overnight, the reaction mixture was concentrated and purified by chromatography (MeOH/AcOEt, 10/90) to afford 115 mg of the chlorin coupled to the protected cyclic peptide. A standard cleavage with a mixture of 0.75 g of crystalline phenol, 0.25 mL of 1,2-ethanedithiol, 0.5 mL of thioanisole, 0.5 mL of deionized H_2O and 10 mL of trifluoroacetic acid (TFA) for 1.5 h afforded the crude peptide, which was lyophilized. The compound was purified by RP-HPLC on a C_{18} semi-preparative column (250×10 mm I.D., Apollo, Alltech) using a 0.1% (v/v) TFA-water/acetonitrile gradient, monitored by both absorbance at 415 nm on a SPD-10A UV–visible detector (Shimadzu) and fluorescence on a RF 10AXL fluorescence detector (Shimadzu).

After removal of the solvents, **2** was lyophilized and kept in the dark in aliquots at −20 °C.

Chemical identities were established by ^{1}H NMR and matrix-assisted laser desorption ionization-time-of-flight MALDI-TOF mass spectrometry, as described previously [16].

^{1}H NMR (DMSO) δ: −1.58, −1.53 (s, 2H, NH-pyrrole), 1.20 (m, 2H, δLys), 1.42 (m, 2H, γArg), 1.53, 1.72 (m, 2H, βArg), 1.55 (m, 2H, δLys), 1.80 (m, 2H, βLys), 2.40, 2.81 (m, 2H, β(D)Phe), 2.84, 2.94 (m, 2H, βAsp), 3.12 (m, 2H, δArg), 4.01 (s, 1H, αLys), 4.08 (s, 2H, Gly), 4.15 (s, 1H, αArg), 4.52 (s, 1H, αAsp), 4.70 (s, 1H, α(D)Phe), 4.13 (s, 4H, CH_2-chlorin), 7.48 (s, 1H, NHε-Arg), 7.65 (s, 1H, NH-Arg), 8.05 (s, 1H, NH-Asp), 8.08 (s, 1H, (D)Phe-NH), 8.12 (s, 1H, NH-Lys), 8.43 (s, 1H, NH-Gly), 7.19–8.84 (m, 30H, ArH, pyrrole), MS (MALDI-TOFMS) *m*/*z*: calculated 1245.55; found: 1246.33.

2.4. Photophysical properties

2.4.1. Absorption and fluorescence

Absorption spectra were recorded on a Perkin-Elmer (Lambda 2, Courtabœuf, France) UV–visible spectrophotometer. Fluorescence spectra were recorded on a SPEX Fluorolog-2 spectrofluorimeter 1680 (Jobin Yvon, Longjumeau, France) equipped with a thermostated cell compartment (25 °C), using a 450 W Xenon lamp.

2.4.2. Determination of singlet oxygen quantum yield ($\Phi(^1O_2)$)

Excitation occurred with a Xe-arc, the light was separated in a SPEX 1680, 0.22 μm double monochromator. The detection at 1270 nm was done through a PTI S/N 1565 monochromator, and the emission was monitored by a liquid nitrogen-cooled Ge-detector model (EO-817L, North Coast Scientific Co). The absorbance of the reference solution (Bengal pink in ethanol solution $\Phi\ ^1O_2) = 0.68$) and the sample solution (at 515 nm) were set equal (between 0.2 and 0.5) by dilution.

2.5. General procedure for in vitro experiments

2.5.1. Cell culture conditions

For *in vitro* experiments, HUVEC, pooled from several donors, were used (Cambrex, Verviers, Belgium). These cells were routinely grown in endothelial growth medium

(EGM-2), containing 2% fetal bovine serum (FBS), growth factors and supplements, and maintained according to the manufacturer's instructions. Only cells from passages 3 to 7 were used for our experiments. Murine mammary carcinoma (EMT-6) cells were grown in 75 cm^2 plastic tissue culture flasks in RPMI 1640 medium supplemented with 9% heat inactivated fetal calf serum, penicillin (100 i.u. mL^{-1}), streptomycin (100 μg mL^{-1}) in an atmosphere of 37 °C and 5% CO_2 atmosphere. Cell culture materials were purchased from Costar (Dutscher, Brumath, France). Cells were subcultured by dispersal with 0.25% trypsin and seeded 5×10^4 cells mL^{-1}. All other chemicals were purchased from Sigma (Saint Quentin Fallavier, France). TPP and the peptidic photosensitizers were dissolved in DMSO at a concentration of 1 mM, aliquoted and kept in the dark.

2.5.2. Expression of $\alpha_v\beta_3$ integrins by flow cytometry analysis

The expression of $\alpha_v\beta_3$ integrins was assessed by flow cytometry. Briefly, after trypsinization, 10^6 cells (HUVEC or EMT-6) were incubated with a monoclonal anti-$\alpha_v\beta_3$ integrin antibody coupled to phycoerythrin (LM609, Chemicon International, Temecula, USA) during 1 h at 4 °C, according to the manufacturer's recommendations. Analysis were performed on 10^4 cells (FACSCalibur, Becton–Dickinson, Meylan, France). Isotype-identical antibodies served as controls.

2.5.3. Dark cytotoxicity

Cell survival after incubation with photosensitizers in the dark was measured using a 3-(4,5-dimethylthiazol-2-yl)-2,5-diphenyl tetrazolium bromide (MTT) assay. Briefly, cells were seeded at the initial density of 1×10^4 cells mL^{-1} in 96-well microtitration plates. TPP and the peptidic photosensitizers were dissolved in DMSO at a concentration of 10^{-3} mol/L, aliquoted and kept in the dark. Forty hours after plating, wells were then emptied, rinsed twice with phosphate buffered saline (PBS) and filled with 200 μL culture media containing various concentrations of photosensitizers (from 0.50 to 10.00 μM). After a 24-h incubation at 37 °C, wells were emptied, rinsed three times with PBS and filled with 200 μL culture media. Cell survival was measured 24 h later, as described previously [17]. Experiments were carried out in triplicates. Results were expressed as relative absorbance to untreated controls. Absorbance values for wells containing medium alone were subtracted from the results of test wells.

2.5.4. Photosensitizers uptake

Cells were seeded at the initial density of 1×10^4 cells mL^{-1} in 96-well microtitration plates. Forty hours after plating, wells were then emptied, rinsed twice with PBS and filled with 200 μL culture media containing various concentrations of photosensitizers for different times, ranging from 1 to 24 h. Medium was then removed, cells were rinsed three times with cold PBS and re-suspended in ethanol and a vigorous pipetting was performed. Photosensitizer was extracted by a 10-min sonication (Branson 1200, Roucaire Instruments Scientifiques, Les Ulis, France). Cell debris were removed by centrifugation (3500*g* for 15 min). Fluorescence (recorded at 650 nm following excitation at 415 nm) was measured on a flx-Xenius spectrofluorimeter (SAFAS, Monaco).

Experiments were carried out at least in triplicates. The fluorescence intensity of each sample was normalized to cell concentration, to molar extinction coefficient values at 415 nm and to fluorescence quantum yield assessed for each compound, respectively.

Experiments were performed with the conjugated chlorins **1**, **2** to only compare the influence of the peptidic moiety on the cellular uptake levels.

2.5.5. Photodynamic activity

Photodynamic activity was assessed by MTT assays. Cell survival was measured 24 h after photosensitization using MTT assay. Cells were seeded at the initial density of 1×10^4 cells mL^{-1} in 96-well microtitration plates. Forty-eight hours after plating, cells were exposed to photo-active compounds at 10^{-6} M. After 24-h incubation at 37 °C, the medium was removed and cells were then washed three times with cold PBS and fresh medium was added before cell irradiation. Results are given as the percentage of the result obtained with the control cultures exposed to photosensitizer alone. Light doses, yielding 50% growth inhibition (LD_{50}), were calculated using medium effect algorithm, and expressed as mean values of three independent experiments performed during different weeks. The dark toxicity of photosensitizers was assessed separately following a similar procedure. Irradiation was carried out at 652 nm, using a diode laser (fluence rate = 2.72 mW cm^{-2}, Coherent, France). Light doses ranged from 1.0 to 11.0 J/cm^2. Negative controls were photosensitizer-free medium without photoirradiation, photosensitizer-free medium with photoirradiation, photosensitizer-containing medium without photoirradiation. Experiments were carried out in triplicates at different days and performed for **1b**, **2** and TPP. Irradiation doses yielding 50% growth inhibition were determined using the medium effect method [20].

2.5.6. Statistical analysis

Mann and Whitney *U*-test was used to test for the significant level between independent variables. The level of significance was set to $P < 0.05$.

3. Results and discussion

3.1. Chemistry

The synthesis of **1** and **1b** have been realized according to a classical Fmoc/*t*-Bu solid-phase methodology. To our knowledge, the synthesis of 5-(4-carboxyphenyl)-10,15,20-triphenylchlorin-cyclo[RGDfK] (**2**) has never been described in literature. It is generally accepted that cyclic RGD peptides display a higher activity compared to the linear counterparts, and this beneficial effect may be due to the fact that the cyclic peptides are conformationally less flexible and metabolically more stable [21,22].

The cyclic pentapeptide c[RGDfK] first designed and synthesised by Kessler and coworkers [23] was selected as a vector because the lysine side chain which is not essential for the activity provides a convenient handle to link the photosensitizer. Different strategies have then been developed to synthesize cyclic pentapeptides containing a RGD sequence. The cyclization can been achieved in solution with the formation of an amide bond [24,25] or by Heck reaction with the formation of a carbon–carbon bond [26]. We can also relate the synthesis of cyclic RGD pseudopeptides containing D-Phe-Ψ[(E)—CHdbondCMe]-L-Val and D-PheΨ[(Z)—CH=CMe]-L-Val type alkene dipeptide isosteres cyclized in solution using DPPA and $NaHCO_3$ [27]. Cyclic hexapeptide that contains a RGD sequence has also been coupled to dimyristoylthioglyceryl anchor using a Fmoc/*t*-Bu chemistry and cyclization with DPPA and $NaHCO_3$ in solution [28].

The cyclization can also been realized on solid phase, and this strategy was described in the work of Wang et al. [29]. They synthesized a fluorescent derivative of the cyclic pentapetide c[KRGDf], by carrying out a cyclization on the solid support in a Boc-Strategy using PyBOP, HOBt and DIEA, deprotecting selectively the lysine side chain and coupling carboxyfluorescein to c[Lys-Arg(Pbf)-Gly-Asp(resin)-Phe] using DIPCDI and HOBt. Another example is given by van Well et al. [30,31]. Cyclic RGD peptides containing either one or two furanoid sugar amino acids have been synthesized by cyclization and the cleavage of the corresponding linear sequence immobilised has been achieved on a solid support *via* the base labile *p*-nitrophenone oxime linker.

To the best of our knowledge, only one example concerning the synthesis of a cyclic RGD peptide coupled to a photosensitizer has been described, by Chaleix et al. [32]. They reported the synthesis of glucosylated porphyrins bearing a cyclic pseudopentapeptide incorporating a RGD sequence obtained by ring-closing metathesis.

For synthesis of **2**, we adapted the improved synthesis based on Kessler's procedure developed by Dai et al. [33]. We chose to couple first in liquid phase the 4-carboxy phenylchlorin (Chl1COOH) to the amine function of the lysine lateral side chain to form the *N*-Fmoc protected lysine modified at the εN position (Scheme 1). Coupling of Fmoc-Lys-OH with *N*-hydroxysuccinimide activated 4-carboxyphenylchlorine afforded Fmoc-Lys(CO-Chl1)-OH. The assembly of the cyclic peptide was achieved on a H-Gly-2-chlorotrityl resin as previously described (Scheme 2). During the coupling of Fmoc-Lys(CO-Chl1)-OH and all the next steps, light exposure was minimized by sealing the reaction vessel in foil to limit the occurrence of unwanted side reactions.

The linear Chl1-CO-RGDfK peptide was cleaved from the resin without affecting other protecting groups with a mixture acetic acid, 2,2,2 trifluoroethane (TFE) and CH_2CL_2 (1/1/3). The head-to-tail cyclization was performed by slowly adding a solution of the linear peptide acetate to a solution of 1-propane-phosphonic acid cyclic anhydride (T3P) in EtOAc (50/50) in the presence of base.

1, **1b**, and **2** were obtained with a final purity greater than 95%, as assessed by analytical RP-HPLC. Two isomers, corresponding to the reduction of a double bond on either opposing side of the tetrapyrrolic macrocycle could be observed by analytical RP-HPLC (data not shown). These isomers arise from the asymmetrical character of the molecule and could also be observed in the commercial TPC used for synthesis. Identities of the compounds were confirmed by MALDI-TOF mass spectrometry and ^1H NMR experiments (Fig. 1A and B).

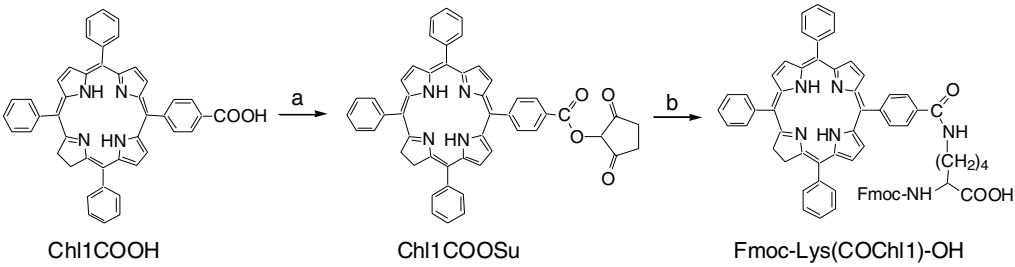

Scheme 1. Preparation of Fmoc-Lys(CO-Chl1)-OH. (a) DCCI, HOSu, CH_2Cl_2, 0 °C, (b) Fmoc-Lys-OH, NMM, DCM, rt.

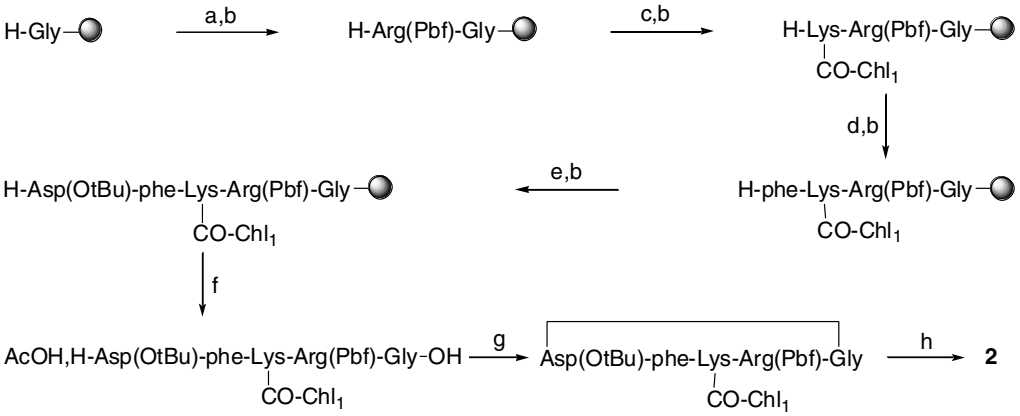

Scheme 2. Synthesis of C-c(RGDfK) **2**. (a) Fmoc-Arg(Pbf)-OH, TBTU, HOBt, DIEA, DMF, (b) 20% piperidine in DMF, (c) Fmoc-Lys(CO-Chl1)-OH, TBTU, HOBt, DIEA, DMF, (d) Fmoc-phe-OH, TBTU, HOBt, DIEA, DMF, (e) Fmoc-Asp(*t*-Bu)OH, TBTU, HOBt, DIEA, DMF, (f) AcOH, TFE, CH_2Cl_2 (1/3/3), (g) 50% 1-propanephosphonic acid cyclic anhydride in EtOAc, TEA, DMAP, CH_2Cl_2, (g) phenol, 1,2-ethanedithiol, thioanisole, deionized H_2O, TFA (6/2/4/4,84).

3.2. Photophysical characteristics

The absorption spectra of **1** and **2** were typical of chlorin derivatives, with a Soret band at about 415 nm and a high extinction coefficient for this signal and four Q bands (516, 543, 598, and 648/650 nm; data not show). In all cases, conjugation induces a decrease in the molar extinction coefficients values, compared to TPP as it has already been observed previously [16,18] (Fig. 1C). The quantum yields of singlet oxygen production ($\Phi(^1O_2)$) for conjugates **1**, **1b**, and **2** were lower than for TPP (Fig. 1C) but still quite high.

3.3. Biological results

3.3.1. Expression of $\alpha_v\beta_3$ integrin by HUVEC and EMT-6 cell lines

The vascular effect can be potentiated by designing photosensitizers localizing primarily in the vascular compartment. Ideally, vascular targeting requires the identification of a target on the surface of angiogenic endothelial cells. Thus, $\alpha_v\beta_3$ integrin is a good candidate for vascular-targeting strategies. In order to validate the use of HUVEC as $\alpha_v\beta_3$-positive cells and EMT-6 line as $\alpha_v\beta_3$-negative cells, integrin expression was investigated. HUVEC strongly expressed $\alpha_v\beta_3$ as assessed by flow cytometry (Fig. 2). No expression was measured for EMT-6 cells. These results confirm that HUVEC express $\alpha_v\beta_3$ integrin which validates their use as an *in vitro* model for our study.

3.3.2. Dark cytotoxicity

A MTT test was used to evaluate the dark cytotoxicity of conjugated photosensitizers and TPP for concentrations ranging from 0.50 to 10.00 μM. A 24-h incubation of the two cell lines in the absence of light exposure with photoactive compounds yielded a surviving cell fraction higher than 85% for concentrations up to 1 μM (data not shown). However,

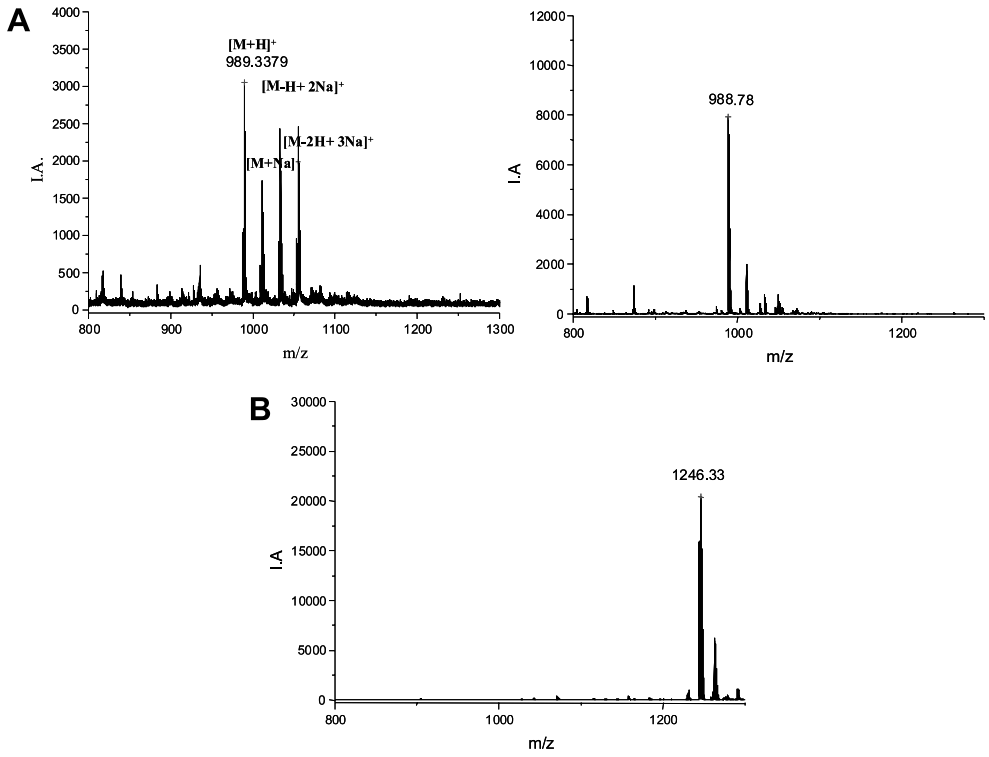

C

	Soret ε_{415}	Q_I $\varepsilon_{648/650}$	Φ ($^1O_2$)
1	19.6	1.80	0.50
1b	136.0	1.52	0.60
2	53.3	5.00	0.75
TPP	556.0	3.40	0.82

Figure 1. (A) MALDI-TOF mass spectra of **1** (left), **1b** (right) and (B) of **2**. (C) molar extinction coefficients (expressed in $10^3\,M^{-1}\,cm^{-1}$) determined at different maximum wavelengths $(\varepsilon)_\lambda$ and singlet oxygen quantum yields Φ ($^1O_2$) of **1**, **1b**, **2** and TPP in EtOH.

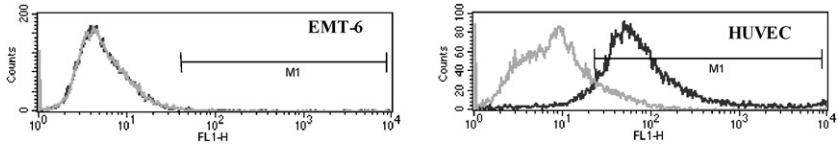

Figure 2. Flow cytometry measurement of $\alpha_v\beta_3$ integrin expression by EMT-6 and HUVEC cells. Cells treated with grey: isotype control. Black: anti- $\alpha_v\beta_3$ coupled to phycoerythrin.

HUVEC showed a higher sensitivity in the dark than the EMT-6 cells which remain viable with concentrations up to 10 μM. All subsequent experiments were carried out at 1.0 μM for both cell lines.

3.3.3. Photosensitizers uptake

The linear relationships between initial concentrations of TPP and conjugates, respectively, in the medium (0.5–10.0 μM), and the amount of photosensitizer after a 24-h incubation period, indicated that the uptake by the two cell lines was dependent on the concentration used and was always higher than TPP (Fig. 3). The cellular uptake of the conjugates **1**, **2** and TPP according to incubation time, was examined in the dark at a non-cytotoxic concentration of 1.0 μM. The accumulation of **1** and **2** was significantly higher $P < 0.05$ than the cellular uptake of TPP from 1 h to 24 h incubation time (Fig. 4). The conjugates accumulated on average 5 times more in HUVEC than in EMT-6 cells. The differences obtained on the different cell lines could be consistent with the dissimilar accumulation of the conjugates expected, if the uptake was receptor mediated.

The cellular uptake of **1** after a 24-h exposure was on average about 98-fold higher than the concentration of TPP and the accumulation of **2** reached 80-fold more, respectively. The intracellular uptake kinetics demonstrated that a steady state was reached at about 15-h exposure (Fig. 4). These results do not confirm that cyclic peptides containing an RGD motif adopt conformations showing a significant increased affinity for integrins [13,14]. It may be noted that accumulation can be related to the dye retention time values (Table 1), higher hydrophobicity (TPP) corresponding to lower uptake. For **1** and **2**, it is not so clear, as the nature of the peptidic moiety could also influence cellular uptake. Nevertheless, improvement of cellular uptake for the conjugated compounds was partly

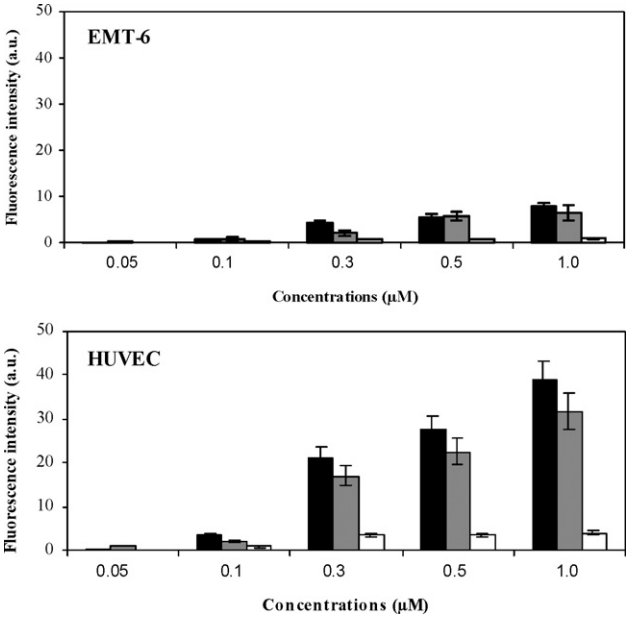

Figure 3. Concentration dependence of the uptake of **1** [black], **2** [grey] and TPP [white, 10-fold increased] in EMT-6 cells and HUVEC. Cells were incubated with photosensitizers for 24 h at concentrations ranging from 0.05 to 1.0 μM. Cellular fluorescence intensities after extraction were measured at 652 nm following excitation at 415 nm. These data represent the mean values from three independent experiments. Errors bars are standard deviations (SD).

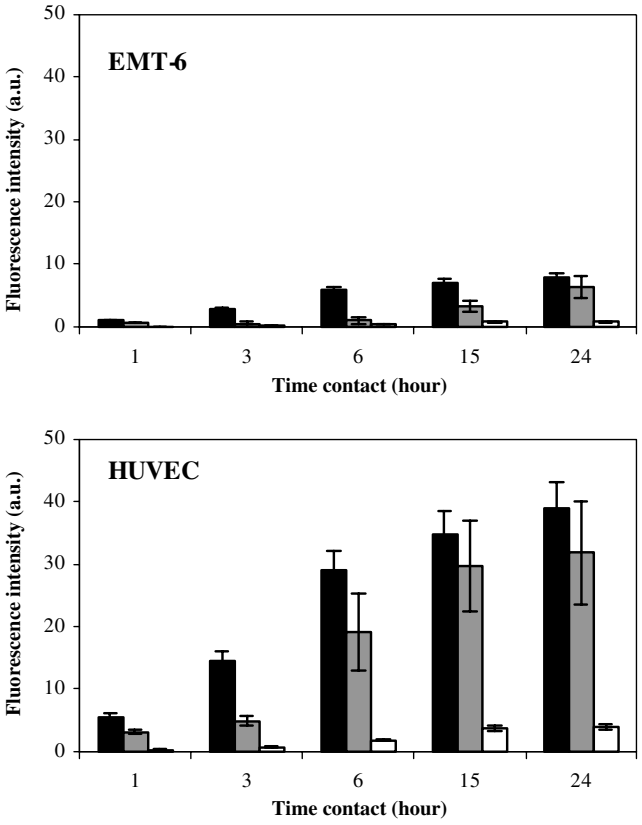

Figure 4. Uptake kinetics of **1** [black], **2** [grey] and TPP [white, 10-fold increased] in EMT-6 cells and HUVEC. Cells were incubated with photosensitizers at 1 μM. Intracellular concentrations were calculated as described in Fig. 3. Data points show the mean ± SD, $n = 3$.

Table 1
Retention times of conjugates **1**, **1b**, **2** and TPP assessed by HPLC

	1	**1b**	**2**	TPP
Retention times (min)	15.10 ± 0.05*	16.4 ± 0.05	17.70 ± 0.05	35.60 ± 0.04
	15.50 ± 0.05		18.20 ± 0.05	

* Mean ± SD, $n = 3$.

related to the increase of their hydrophilicity (Table 1). Thus, peptidic moiety also led to a non-specific increased cellular uptake by EMT-6 cells, lacking RGD binding receptors (Fig. 4, EMT-6). These results suggest that a part of the increased uptake of conjugates was related to non-specific mechanisms. Actually, most photosensitizers are hydrophobic, highly adsorptive, and tend to aggregate in aqueous media as a result of the propensity of the hydrophobic skeleton to avoid contact with water molecules [34]. In our *in vitro* experimental conditions, photosensitizers could not be diluted in compatible biological medium without forming insoluble aggregates, which could increase uptake in an aspecific manner, through passive diffusion or endocytosis of aggregated photosensitizer molecules,

depending on photosensitizer chemical structure and hydrophobicity [35]. Aspecific uptake was also evidenced in our previous work with photosensitizer conjugated to ATWLPPR [18].

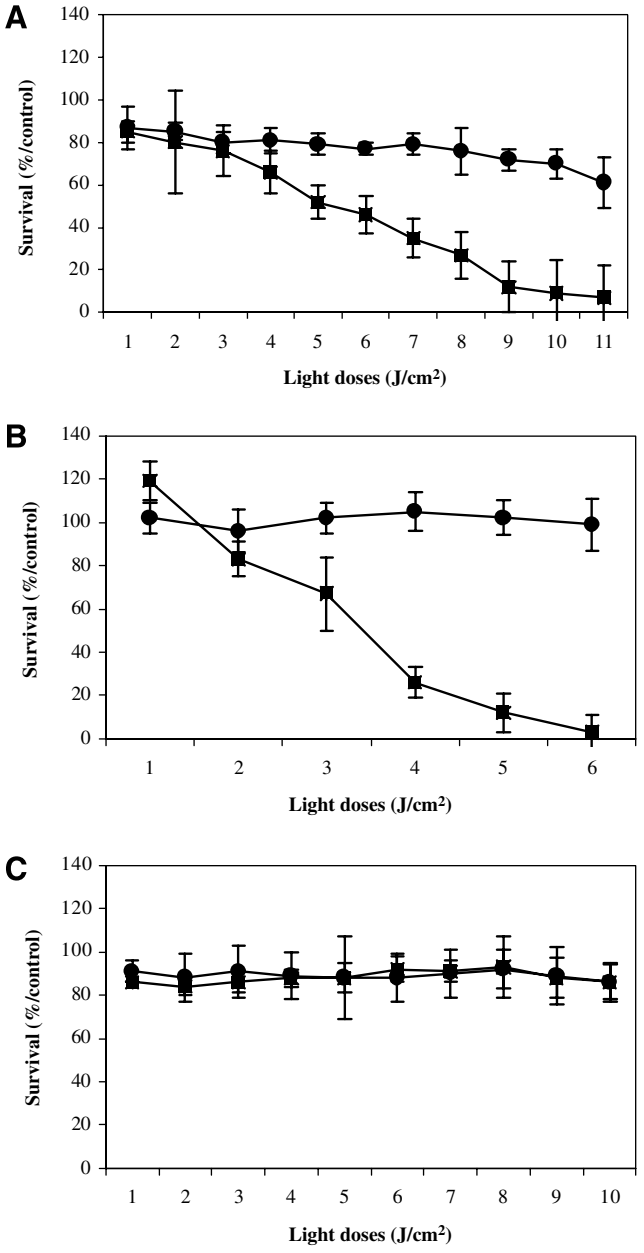

Figure 5. Measurement of photodynamic therapy sensitivity to conjugated photosensitizers with linear peptide **1b** (A), cyclic peptide **2** (B) and TPP (C) in HUVEC [square] and EMT-6 cells [circle]. Cells were incubated with photosensitizers at 1 μM for 24 h before light treatment. Survival curves, obtained by MTT, were obtained for cells exposed to increasing doses of light from 1.0 to 11.0 J/cm^2 (data points show the mean ± SD, $n = 3$).

3.3.4. Photodynamic activity

HUVEC and EMT-6 cells were incubated with the photo-active compounds at 1 μM and irradiated by red light. Because one aim of this work was to improve photosensitization to red light, which is a light wavelength able to enter deeply in living tissues, we compared the activity of conjugates with TPP. The LD_{50} values of photosensitizers with linear **1b** and cyclic peptide **2** were comparable with 3.8 and 3.1 J/cm^2, respectively (Fig. 5A and B). Fig. 5C shows that TPP control photosensitizer displayed no photocytotoxicity in our experimental conditions in HUVEC and EMT-6 cells. Conversely, survival measurements demonstrated that using conjugated compounds, the photosensitivity was not improved for EMT-6 cells (Fig. 5A and B). In HUVEC positive cells, the lowest uptake observed for TPP is consistent with the lack of photosensitivity and the most pronounced photodynamic activity measured for conjugated photosensitizers is in relation with the improvement of cellular uptake in the presence of peptidic moiety. Chaleix et al. reported the solid-phase synthesis of four porphyrins bearing the $\alpha_v\beta_3$ integrin ligand RGD [32]. Three of the conjugates prepared displayed photodynamic activity on the K562 leukemia cell line to a degree comparable to that of Photofrin II®. The authors later described the synthesis of a cyclic peptide containing the RGD motif and adopting conformations showing an increased affinity for integrins [36]. In the ring closing metathesis method used for synthesis, the enzymatically-sensitive disulfide bond of the cyclic[CRGDC] thiopeptide previously described, is replaced by a carbon–carbon double bond in order to increase the plasmatic lifetime of the peptide. A low substituted resin (0.1 mmol/g) was used in order to avoid intermolecular reactions and thus to increase the reaction yield. Carboxy-glucosylporphyrins coupled to this peptide *via* a spacer arm showed the same efficiency for $^1O_2$ production as hematoporphyrin but to the best of our knowledge, no *in vitro* study on these compounds has been reported yet.

In conclusion, we have used a convenient and simple synthetic pathway to prepare a new family of peptidic photosensitizers with cyclic[RGDfK] RGD motif. The higher photodynamic efficiency has been related to conjugates greater cellular uptake. Our results also show that peptidic moiety is obviously an interesting means to introduce such a balance between hydrophilicity and hydrophobicity, previous observations suggesting the requirement of amphiphilicity for efficient photodynamic activity [37]. RGD-containing linear or cyclic peptide targeted tetraphenychlorin or tetraphenylporphyrin are much more potent photosensitizers that unconjugated photosensitizer in HUVEC over-expressing $\alpha_v\beta_3$ integrin. According to our *in vitro* results, photosensitizers with linear or cyclic RGD motif could comparatively target tumor endothelial cells and may efficiently potentate the vascular effect of PDT *in vivo*.

Acknowledgments

This work was supported by the research funds of the French "Ligue Nationale Contre le Cancer, Comités Lorrains" and "La Région Lorraine".

References

[1] T. Patrice, D. Olivier, L. Bourre, J. Environ. Pathol. Toxicol. Oncol. 25 (2006) 467–486.
[2] T.J. Dougherty, Photochem. Photobiol. 45 (1987) 879–889.

[3] T.J. Dougherty, C.J. Gomer, B.W. Henderson, G. Jori, D. Kessel, M. Korbelik, J. Moan, Q. Peng, J. Natl. Cancer Inst. 90 (1998) 889–905.
[4] W.M. Sharman, J.E. van Lier, C.M. Allen, Adv. Drug Deliv. Rev. 56 (2004) 53–76.
[5] J. Folkman, Nat. Med. 1 (1995) 27–31.
[6] K. Ichikawa, T. Hikita, N. Maeda, S. Yonezawa, Y. Takeuchi, T. Asai, Y. Namba, N. Oku, Biochim. Biophys. Acta 1669 (2005) 69–74.
[7] G. Poste, G.L. Nicolson, Biomembranes 11 (1983) 341–364.
[8] A. Bamias, M.A. Dimopoulos, Eur. J. Int. Med. 14 (2003) 459–469.
[9] F.G. Giancotti, E. Ruoslahti, Science 285 (1999) 1028–1032.
[10] A. van der Flier, A. Sonnenberg, Cell Tissue Res. 305 (2001) 285–298.
[11] P.C. Brooks, R.A. Clark, D.A. Cheresh, Science 264 (1994) 569–571.
[12] R. Haubner, H.J. Wester, Curr. Pharm. Des. 10 (2004) 1439–1455.
[13] R. Haubner, H.-J. Wester, W.A. Weber, C. Mang, S.I. Ziegler, S.L. Goodman, R. Senekowistsch-Schmidtke, H. Kessler, M. Schwaiger, Cancer Res. 61 (2001) 1781–1785.
[14] N. Assa-Munt, X. Jia, P. Laakkonen, R. Ruoslahti, Biochemistry 40 (2001) 2373–2378.
[15] G.C. Tucker, Curr. Oncol. Rep. 8 (2006) 96–103.
[16] B. Di Stasio, C. Frochot, D. Dumas, P. Even, J. Zwier, A. Müller, J. Didelon, F. Guillemin, M.L. Viriot, M. Barberi-Heyob, Eur. J. Med. Chem. 40 (2005) 1111–1122.
[17] R. Schneider, F. Schmitt, C. Frochot, Y. Fort, N. Lourette, F. Guillemin, J.F. Muller, M. Barberi-Heyob, Bioorg. Med. Chem. 13 (2005) 2799–2808.
[18] L. Tirand, C. Frochot, R. Vanderesse, N. Thomas, E. Trinquet, S. Pinel, M.L. Viriot, F. Guillemin, M. Barberi-Heyob, J. Control. Release 11 (2006) 153–164.
[19] J. Neimark, J.P. Briand, Pept. Res. 6 (4) (1993) 219–228.
[20] T.C. Chou, P. Talalay, Adv. Enzyme Regul. 22 (1984) 37–64.
[21] A. Giannis, T. Kolter, Angew Chem. Int. Ed. Engl. 32 (1993) 1244–1267.
[22] S.J. Bogdanowich-Knipp, S. Chakrabarti, T.D. Williams, R.K. Dillman, T.J. Siahaan, J. Pept. Res. 53 (1999) 530–541.
[23] R. Haubner, W. Schmitt, G. Hölzemann, S.L. Goodman, A. Jonczyk, H. Kessler, J. Am. Chem. Soc. 118 (1996) 7881–7891.
[24] C.F. McCusker, P.J. Kocienski, F.T. Boyle, A.G. Schätzlein, Bioorg. Med. Chem. Lett. 12 (2002) 547–549.
[25] D. Boturyn, P. Dumy, Tetrahedron Lett. 42 (2001) 2787–2790.
[26] K. Akaji, K. Teruya, M. Akaji, S. Aimoto, Tetrahedron 57 (2001) 2293–2303.
[27] S. Oishi, T. Kamano, A. Niida, Y. Odagaki, N. Hamanaka, M. Yamamoto, K. Ajito, H. Tamamura, A. Otaka, N. Fujii, J. Org. Chem. 67 (2002) 6162–6173.
[28] B. Hu, D. Finsinger, K. Peter, Z. Guttenberg, M. Bärmann, H. Kessler, A. Escherich, L. Moroder, J. Böhm, W. Baumeister, S.f. Sui, E. Sackmann, Biochemistry 39 (2000) 12284–12294.
[29] W. Wang, Q. Wu, M. Pasuelo, J.S. McMurray, C. Li, Bioconjug. Chem. 16 (2005) 729–734.
[30] R.M. van Well, H.S. Overkleeft, M. Overhand, E.V. Carstenen, G.A. van der Marel, J.H. van Boom, Tetrahedron Lett. 41 (2000) 9331.
[31] R.M. van Well, H.S. Overkleeft, G.A. van der Marel, D. Bruss, G. Thibault, P.G. de Groot, J.H. van Boom, M. Overhand, Bioorg. Med. Chem. Lett. 13 (2003) 331–334.
[32] V. Chaleix, V. Sol, M. Guilloton, R. Granet, P. Krausz, Tetrahedron Lett. 45 (2004) 5295–5299.
[33] X. Dai, Z. Su, J.O. Liu, Tetrahedron Lett. 41 (2000) 6295–6298.
[34] I. Rosenthal, Photochem. Photobiol. 53 (1991) 859–870.
[35] R. Schneider, L. Tirand, C. Frochot, R. Vanderesse, N. Thomas, J. Gravier, F. Guillemin, M. Barberi-Heyob, Curr. Med. Chem. Anti-Cancer Drugs 6 (2006) 469–488.
[36] V. Chaleix, V. Sol, Y.M. Huang, M. Guilloton, R. Granet, J.C. Blais, P. Krausz, Eur. J. Org. Chem. 8 (2003) 486–1493.
[37] A.S. Sobolev, D.A. Jans, A.A. Rosenkranz, Prog. Biophys. Mol. Biol. 73 (2000) 51–90.